“Lift Coefficient for an Airfoil”

by

David M. Smiadak

School of Engineering

Grand Valley State University

EGR 365 – Fluid Mechanics

Instructor: Dr. M. Sözen

July 15, 2008

1.0 Purpose

The purpose of this laboratory experiment was to experimentally measure the pressure distribution over a Clark Y-14 Airfoil and to determine the lift coefficient at a particular angle of attack.

2.0 Background/Theory

An airfoil develops lift at positive angles of attack through lower pressures over the top of the airfoil compared to pressures under the airfoil. The lift and drag coefficients are strongly dependent on angle of attack and less dependent on Reynolds number. Reynolds number effects are particularly important in the region of maximum lift coefficient just prior to stall.) The lift force can be found from the lift coefficient, CL, in the following way,

$$L = \frac{1}{2}\rho A V^2 CL \tag{1}$$

where ρ is the density of the fluid through which the airfoil moves, A is the area equal to the span times the mean chord of the airfoil, V is the undisturbed flow speed, CL is the lift coefficient, and L is the lift force. The airfoil and the corresponding flow around it are shown in Figure 2.1.

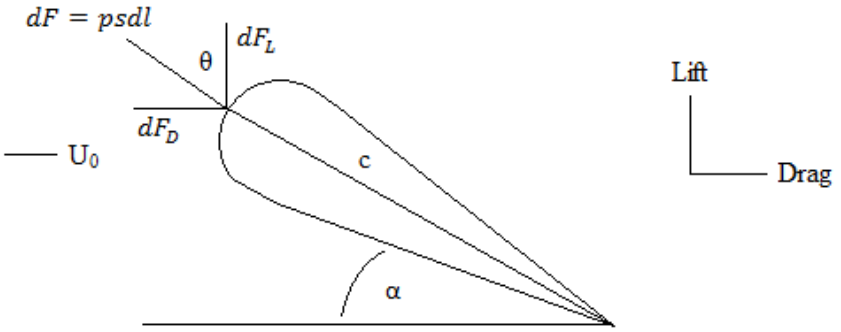

Figure 2.1: Clark Y-14 Airfoil

Although the emphasis in this lab is on the lift coefficient, the lift to drag ratio is often of interest to the designer since it represents a kind of aerodynamic efficiency-the most economical cruising condition for an airplane is determined from the point of maximum lift to drag ratio. It is also

used to select the velocity and angle of attack for maximum range in a power-off condition. This is of obvious importance to a pilot attempting to land after an engine failure and is always important to a glider pilot.

Forces on the airfoil can be found by direct measurement if the airfoil is mounted on a force balance. Forces can also be found by integrating the pressure distribution over the surface of the wing. In this lab, the integrated pressure distribution will be used. The airfoil mounted in the wind tunnel is equipped with 18 pressure openings located at 0, 7.5, 10, 20, 30, 40, 50, 60, and 70 percent chord on both the upper and lower surfaces. There is an additional opening at 80 percent of chord on the upper surface. Pressures relative to the static pressure in the wind tunnel can be measured using the scani-valve. The pressure coefficient can be expressed by,

$$C_p = \frac{p - p_\infty}{\frac{1}{2}\rho U_0^2} \tag{2}$$

The lift of the airfoil can be expressed as,

$$Lift = F_L = \iint_{surface} dF_L = \left[\int_0^L dF\ cos\theta\right]_{top} + \left[\int_0^L dF\ cos\theta\right]_{bottom}$$

For simplicity this span is considered uniform, because of this, integration is only necessary over L giving,

$$\int_0^L dF cos\theta = \int_0^L ps\ dl\ cos\theta = \int_0^L (p - p_\infty) s\ dl\ cos\theta$$

It is known that $cos\theta = \frac{dx}{dl}$ yielding,

$$\int_0^L (p - p_\infty) s\ dl\ \frac{dx}{dl} = s\int_0^L (p - p_\infty) dx$$

With the distance along the chord defined as $dx = dc(cos\alpha)$,

$$s\int_0^L (p - p_\infty)\cos\alpha \, dc = F_L$$

It is known from equation (1) that,

$$C_L = \frac{F_L}{\frac{1}{2}\rho U_o^2 A}$$

Substituting in for F_L yields,

$$C_L = \frac{(s\cos\alpha)}{\frac{1}{2}\rho U_o^2 A} \cdot \int_0^L (p - p_\infty) dc$$

$$C_L = \frac{(s\cos\alpha)}{s \cdot c} \cdot \int_0^L \frac{(p - p_\infty)}{\frac{1}{2}\rho U_0^2} dc$$

Substituting in the coefficient of pressure yields,

$$C_L = \left[\frac{(\cos\alpha)}{c} \cdot \int_0^L C_p \, dc\right]_{(top\ to\ bottom)}$$

3.0 Results and Discussion

The pressure readings taken for 0°, 7°, and 14° are shown in Table 3.1.

Table 3.1: Experimental results, three angles of attack

	Pressure Reading		
Port	**Inches of H_20, 0°**	**Inches of H_20, 7°**	**Inches of H_20, 14°**
1	-1.26	-1.09	-1.27
2	-2.14	-2.08	-1.28
3	-2.49	-2.96	-1.4
4	-2.77	-3.48	-2.52
5	-3.15	-4.35	-4.37
6	-3.35	-5.61	-6.13
7	-3.63	-6.31	-8.01
8	-3.34	-7.34	-10.23
9	-2.42	-8.32	-14.63
10	3.66	1.1	-4.72
11	-3.61	1.23	3.89
12	-1.82	0.81	2.35
13	-0.36	0.87	1.92
14	-0.28	0.73	1.63
15	-0.14	0.69	1.27
16	-0.01	0.61	0.97
17	0.06	0.54	0.71
18	0.13	0.42	0.42

Ports 1 through 9 are located on the top of the airfoil, port 10 is located on the leading edge of the airfoil and ports 11 through 18 are located on the bottom of the airfoil at the percent increments described in the Background/Theory section.

The pressure coefficients are then determined for each point along the airflow and plot in Figure 3.1 for an attack angle of 0°.

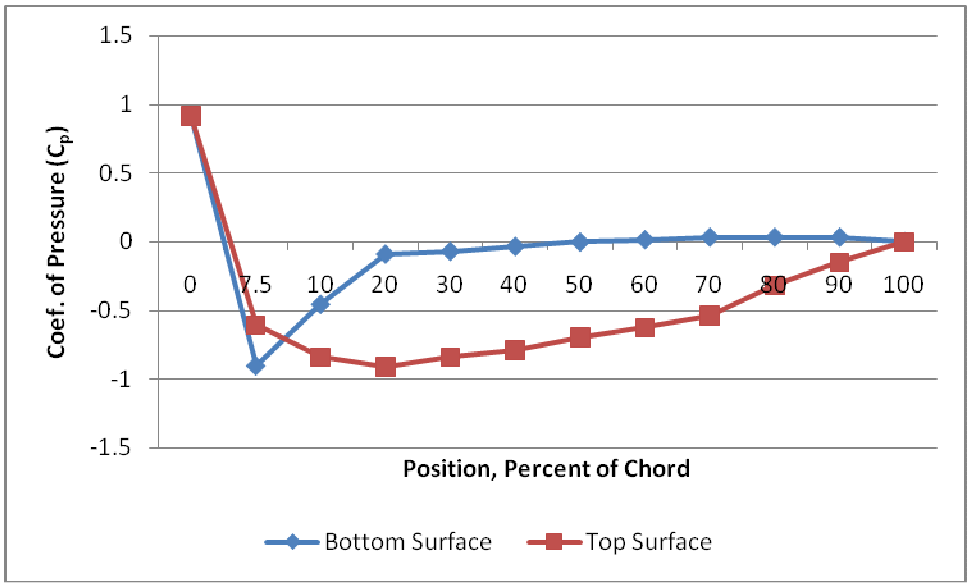

Figure 3.1: Pressure Coefficients, attack angle of 0°

A sample calculation for the pressure coefficient is shown. First the pressure recorded in inches of water is converted to pounds per square foot,

$$-1.26\ in.of\ H_2O\left|\frac{1\ ft}{12\ inches}\right|\left(62.4\frac{lb}{ft^3}\right) = -6.552\ psf$$

Then using equation (2), the pressure coefficient for that port can be determined,

$$C_p = \frac{-6.552\ psf}{\frac{1}{2}\left(2.38x10^{-3}\frac{slugs}{ft^3}\right)\left(132\ \frac{ft}{s}\right)^2} = -0.31599$$

The pressure coefficients are then determined for a 7° angle of attack Figure 3.2.

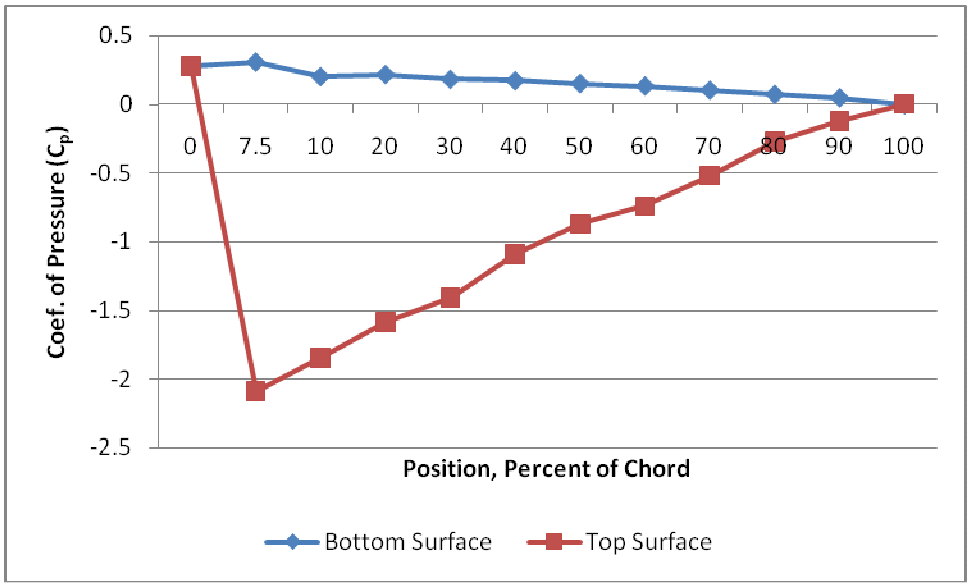

Figure 3.2: Pressure Coefficients, attack angle of 7°

The pressure coefficients for a 14° angle of attack are shown in Figure 3.3.

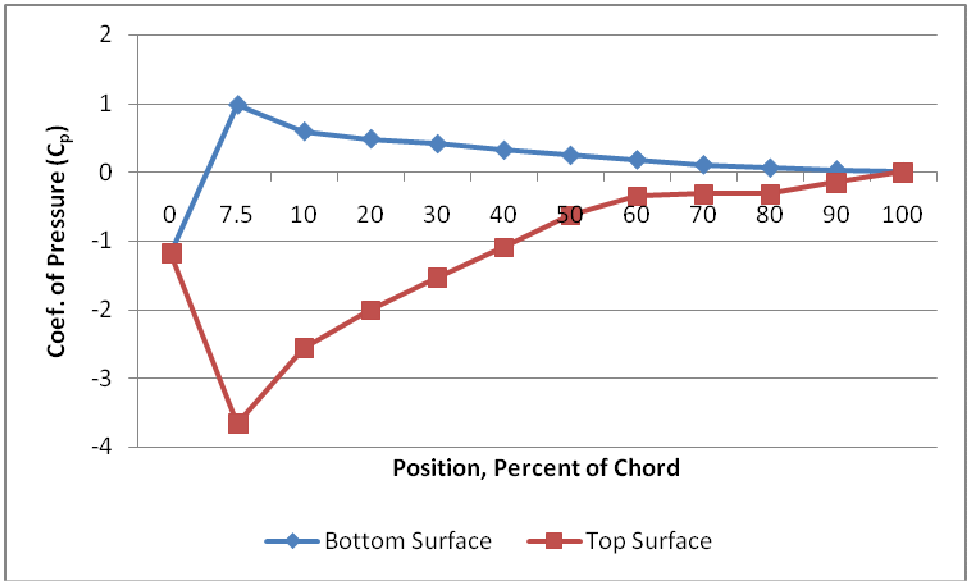

Figure 3.3: Pressure Coefficients, attack angle of 14°

The coefficients of lift for each trial were then determined using the midpoint approximation technique. The tables and sample calculations for this approximation are shown in Appendix 5.1. The experimental data collected for all three angles of attack were extrapolated out to cover 100% of the chord length for complete analysis over the entire airfoil.

3.1 FlowLab Results

The FlowLab results for a 0˚ attack angle are shown in Figure 3.4.

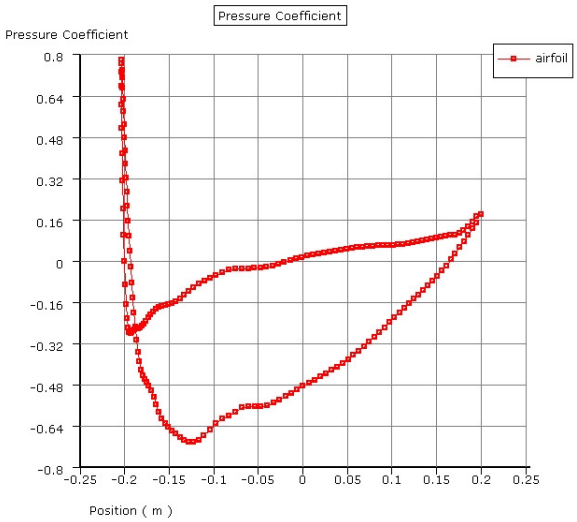

Figure 3.4: Pressure Coefficients, attack angle of 0°

The FlowLab results for a 7˚ attack angle are shown in Figure 3.5.

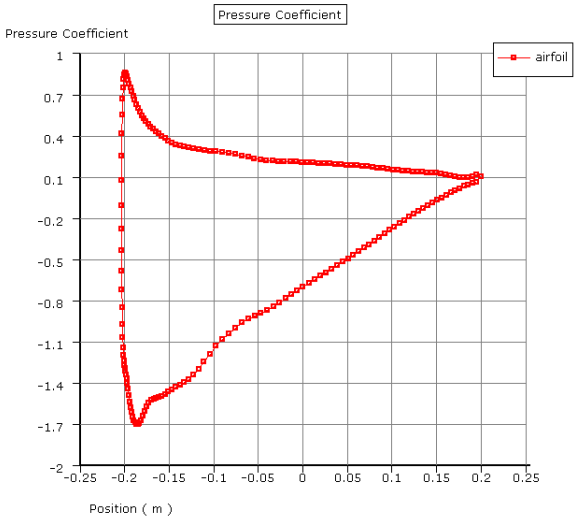

Figure 3.5: Pressure Coefficients, attack angle of 7˚

Finally the FlowLab results for a 14˚ attack angle are shown in Figure 3.6.

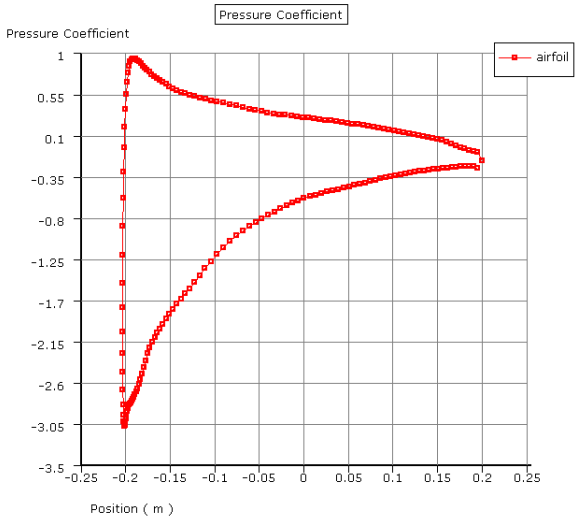

Figure 3.6: Pressure Coefficients, attack angle of 14˚

The coefficients of lift and drag determined from FlowLab are shown below in Table 3.2.

Table 3.2: FlowLab Coefficients of Lift and Drag

	Angle of Attack		
	0°	7°	14°
Coefficient of Lift	0.36324	0.990493	1.23876
Coefficient of Drag	0.0103178	0.0366205	0.117959

The FlowLab results are then compared to the experimentally determined coefficients of lift in Table 3.3.

Table 3.3: Coefficient of Lift comparison

Angle of Attack	Experimental	FlowLab	Percent Discrepancy
0°	0.487	0.363	33.963
7°	1.011	0.990	2.045
14°	1.216	1.239	1.831

A sample calculation for the percent discrepancy is shown below,

$$percent\ discrepancy = \frac{\left| f_{theoretical} - f_{experimental} \right|}{f_{theoretical}} \cdot 100\%$$

$$percent\ discrepancy = \frac{|1.239 - 1.216|}{1.239} \cdot 100\% = 1.831\%$$

3.2 Error Analysis

The largest source of error when determining the experimental coefficients of lift was recording the correct pressure values at each port. From the expression below, propagated error analysis can be performed.

$$C_L = \left[\frac{(cos\alpha)}{c} \cdot \int_0^L C_p\, dc\right]_{(top\ to\ bottom)}$$

$$U_{CL} = CL\sqrt{\left(\frac{U_{\Delta p}}{\Delta p}\right)^2 + 4\left(\frac{U_U}{U}\right)^2}$$

For an angle of attack of 0˚,

$$U_{CL} = 0.487\sqrt{\left(\frac{0.005in}{-1.26in}\right)^2 + 4\left(\frac{0.5\frac{ft}{s}}{132\frac{ft}{s}}\right)^2}$$

$$U_{CL} = 0.0041$$

From this value of uncertainty it can be determined that the propagated error present in the coefficient of drag equation is negligible.

4.0 Conclusions

In conclusion, the experimentally determined results accurately reflected the theoretical results determined by FlowLab simulations of a Clark Y-14 airfoil. The percent discrepancy between the experimental and FlowLab results for the lift coefficients were acceptable and it was concluded that a Clark Y-14 airfoil can be accurately modeled in a wind tunnel environment to determine coefficients of lift.

5.0 Appendices

5.1 Coefficient of Lift Approximations

6.0 References

1. Fleischmann, Shirley. *Fluid Mechanics EGR 365 Designed-Based Fluids Lab.* Grand Rapids: Grand Valley State University, 2005.

2. Munson, Young, and Okiishi. *Fundamentals of Fluid Mechanics, Fifth Edition.* Hoboken: John Wiley & Sons, Inc.